Breakdown of a Mott Insulator: A Nonadiabatic Tunneling Mechanism

Takashi Oka, Ryotaro Arita, and Hideo Aoki
Department of Physics, University of Tokyo, Hongo, Tokyo 113-0033, Japan
(Received 26 March 2003; published 5 August 2003)

Time-dependent nonequilibrium properties of a strongly correlated electron system driven by large electric fields is obtained by means of solving the time-dependent Schrödinger equation for the many-body wave function numerically in one dimension. While the insulator-to-metal transition depends on the electric field and the interaction, the metallization is found to be described in terms of a universal Landau-Zener quantum tunneling among the many-body levels. These processes induce current oscillation for small systems, while giving rise to finite resistivity through dissipation for larger systems/on longer time scales.

DOI: 10.1103/PhysRevLett.91.066406 PACS numbers: 71.30.+h, 71.27.+a

Introduction.—Nonlinear responses and time-dependent phenomena are an open frontier in the physics of strongly correlated systems. Properties beyond the linear-response or time-dependent properties have been much discussed [1], but remain a challenging problem, which is, theoretically, due to the difficulty in dealing simultaneously with the many-body effect (correlation) and finite current (nonequilibrium), which are both nonperturbative physics.

In this Letter, we consider the Hubbard model under constant driving forces in one dimension. The ground state of the half-filled Hubbard system is a Mott insulator [2] for arbitrary strengths of the electron-electron repulsion $U > 0$, while the state is metallic when the band filling is shifted away from the half-filling by doping carriers. So the question we pursue here is the following: what will happen if we destroy the Mott insulator by applying strong electric field, instead of doping?

There are existing theoretical approaches that employ the Bethe ansatz method, and the closing of the Mott gap has been discussed [3,4]. In these studies, however, electric fields are not actually applied, but the left-going and right-going hopping terms are made different instead. It is rather difficult to relate this artificial, and non-Hermitian, model with a system in an electric field. That is why we have here opted for actually applying electric fields for the first time to keep track of the time evolution of the many-body wave functions and levels. For that we make use of a numerical integration of the time-dependent Schrödinger equation.

We have found that the electric field, if strong enough, breaks the Mott-insulator phase. While the critical field strength required for the breakdown of the Mott insulator depends sensitively on the magnitude of the electron-electron interaction, we propose here that the mechanism for the metallization can be viewed as the nonadiabatic tunneling between the many-body levels. We have verified this by confirming numerically that a universal Landau-Zener quantum tunneling governs the nonlinear conduction, where the fit is surprisingly good although the Landau-Zener formalism is originally intended for one-body problems while the problem at hand, being many-body, involves the Hilbert space with huge dimensions.

Just after the metallization, we have a self-induced current oscillation. While this should be realistic for mesoscopic systems, for large systems or on a longer time scale, a novel, "Ohmic" conduction is found to result. This occurs despite the absence of disorder and the heat bath degrees of freedom, but a series of nonadiabatic tunneling among many-body states is responsible for the dissipation effect. Indeed, the breakdown of a one-dimensional (1D) [5] as well as two-dimensional (2D) [6] Mott insulator has been experimentally studied, and, among other interesting phenomena including spontaneous density-pattern formations [5–7], a seemingly Ohmic conduction was found for a rather wide range of external electric field, until the Ohmic conduction is eventually broken.

Formulation.—To get rid of ambiguities arising from the electrodes, we have opted here for a periodic system (a ring in 1D), where the electric field F is applied via a time-dependent AB flux $\Phi(t) = eLFt$ piercing the ring [inset of Fig. 1(a); L, sample length]. This will lead to a circular electromotive force due to Faraday's law. The flux makes the hopping integral in a tight-binding model complex, where the Hamiltonian is

$$H(t) = -\frac{W}{4}\sum_{i,\sigma}[\, e^{2\pi i\Phi(t)/N} c^{\dagger}_{i+1\sigma} c_{i\sigma} + \text{h.c.}\,] + U\sum_{i} n_{i\uparrow} n_{i\downarrow}. \tag{1}$$

Here W is the bandwidth, U the electron-electron repulsion, and $N = L/a$ the total number of sites with a being the lattice constant. Hereafter we take the unit in which $e = a = h = 1$.

We have then to solve the time-dependent Schrödinger equation, $i\frac{d}{dt}|\Psi(t)\rangle = H(t)|\Psi(t)\rangle$, which governs time evolution of the quantum system at absolute zero temperature, starting from the ground state of the Hamiltonian at $t = 0$, $|\Psi(t = 0)\rangle \equiv |\Psi_0\rangle$, which is obtained with the Lanczos method. The time integration of the

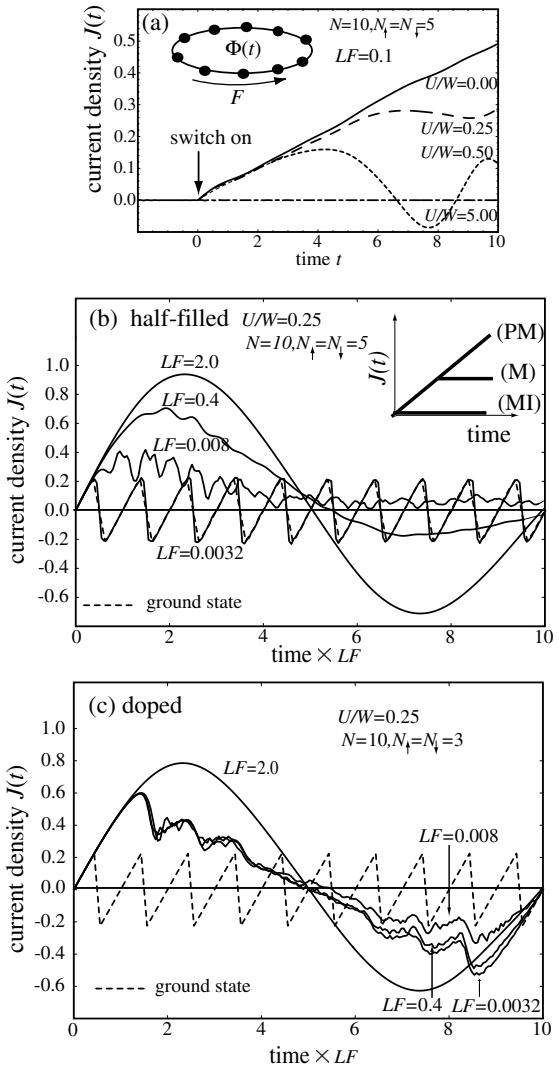

FIG. 1. (a) Time evolution of the current, $J(t)$, for a half-filled, 10-site Hubbard model for various strengths of the correlation, $0 \le U/W \le 5$, for a fixed electric field $F = 1/10L$. Time is measured in units of $\tau_W \equiv 4\hbar/W$, LF in $W/(4\hbar)$, and $J(t)$ in $1/\tau_W$. The range of the time in this panel corresponds to a range of the AB flux $0 \le \Phi/\Phi_0 \le 1$. The inset schematically depicts the sample geometry, where an AB flux, $\Phi(t) = LFt$, increasing linearly with time induces an electric force through Faraday's law. (b) A longer-time behavior of the current when F is varied with a fixed $U/W = 0.25$, again for the half-filled case. Here the horizontal axis is $LFt = \Phi(t)/\Phi_0$ and over $0 \le \Phi/\Phi_0 \le N(= 10$ here). The inset schematically shows three kinds of behavior: MI, Mott insulator; M, metal; PM, perfect metal. (c) A plot similar to (b) for a non-half-filled case ($N_\uparrow = N_\downarrow = 3 < N/2 = 5$).

state vector, which, being many-body, has a huge dimension, requires a reliable algorithm. So we adopt here Cranck-Nicholson's method [8] that guarantees the unitary time evolution, where the time evolution is put in a form, $|\Psi(t + \Delta t)\rangle = e^{-i\int_t^{t+\Delta t} H(t)\, dt}\, |\Psi(t)\rangle \simeq [1 - i\Delta t/2H(t + \Delta t/2)]/[1 + i\Delta t/2H(t + \Delta t/2)]\, |\Psi(t)\rangle$, which is unitary by definition. Here the time step is taken to be small enough ($dt = 1.0 \times 10^{-2}$ with the time in units of $4\hbar/W$ hereafter) to ensure convergence for $N \le 10$ site systems, for which the dimension of the Hamiltonian is $\sim 10^4$. We have concentrated on the total $S^z = 0$ subspace with $N_\uparrow = N_\downarrow = N/2$.

Result.—We first plot in Fig. 1(a) the result for the expectation value of the current density averaged over the sites,

$$J = -\frac{W}{4N}\sum_{i,\sigma}(ie^{2\pi i\Phi/N}\, c^\dagger_{i+1\sigma}c_{i\sigma} + \text{h.c.}). \qquad (2)$$

The behavior of $J(t)$ for various values of U with a fixed value of the electric field F is seen to fall upon three regimes when U is varied: A perfect metallic behavior [$J(t) \propto t$] when the electrons are free ($U/W = 0$), while when the interaction is strong enough ($U/W \gg 1$) the current has a zero expectation value. For an intermediate regime of U/W we have finite J's with some oscillations in the current for finite systems. By contrast, a non-half-filled system has the time evolution distinct from the ground-state behavior. The difference has its root in the spectral property as will be discussed later.

Now, Fig. 1(b) plots the time evolution of the current when the electric field F is varied with a fixed value of U/W, again for the half-filled case. The result may be summarized as follows:

(i) Small F regime (Mott insulator): A drastic difference between the half-filled and doped systems appears for small F. When half-filled, $J(t)$ in the limit of $F \to 0$ smoothly approaches the $\langle J(t)\rangle = 0$ behavior of the ground state (Mott insulator). Here $\langle J(t)\rangle$ is the time-averaged current. On top of the $\langle J(t)\rangle = 0$ an oscillatory behavior with the period of $\Phi_0 (\equiv e/h = 1$: flux quantum) is seen, which is nothing but the AB oscillation (a sawtooth, due to a symmetry about $\Phi = \Phi_0/2$).

(ii) Moderate F regime (metal): In this regime, the current in the half-filled case shows an oscillatory behavior [see typically the $LF = 0.008$ data in Fig. 1(b)].

(iii) Large F regime (perfect metal): When the electric field F becomes large enough, the system becomes a metal, in which $\langle J(t)\rangle \propto t$ for $\Delta\Phi < \Phi_0 N/4$. A further oscillation in $J(t)$, with a long period ($\Delta\Phi = \Phi_0 N$), is seen, which we will discuss later.

The F dependence of $\langle J\rangle$ is displayed in Fig. 2 as the I-V characteristics for various values of U. Here the time average $\langle J\rangle = \int_0^{\Delta t}\langle J(t)\rangle dt/\Delta t$ ($LF\Delta t = N\Phi_0/4$) of the current density $J(t)$ is taken over one-fourth of the extended AB period ($0 \le \Phi \le N\Phi_0/4$), since we are interested in the rise in the current which should represent the behavior in the thermodynamic limit. We can see that $\langle J\rangle$ becomes nonzero rather abruptly at the metallization, where the threshold electric field increases with U/W, thereby the F dependence becoming weaker. Just after the metallization some oscillation (in the F dependence this time) is seen for finite systems.

Nonadiabatic tunneling.—In order to understand the physics underlying these time evolutions and their F

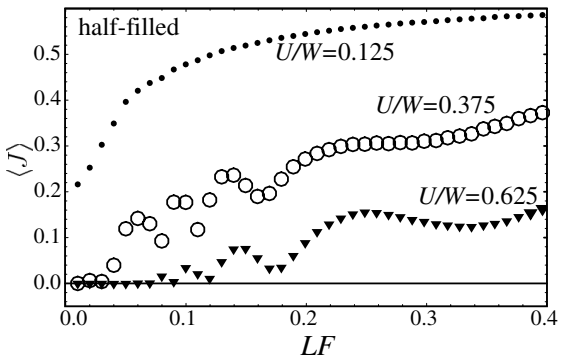

FIG. 2. I-V characteristics for various values of U/W for the half-filled Hubbard model with $N = 6$.

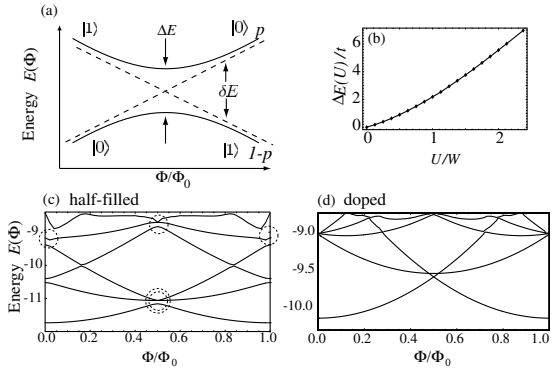

FIG. 3. (a) Landau-Zener process around a level anticrossing, where ΔE denotes the gap, p the transition probability, and δE the difference between the "unperturbed," crossing energy levels (dashed lines). (b) U dependence of the many-body gap ΔE marked with a double circle in (c). (c) The low-lying levels versus Φ for the Hamiltonian Eq. (1) in the half-filled case ($N = 10$ with $N_\uparrow = N_\downarrow = 5$) for $U/W = 0.125$. Level repulsions due to the interaction U are encircled. (d) A similar plot for a doped case ($N = 10$ with $N_\uparrow = N_\downarrow = 3$).

dependences, let us here evoke the notion of nonadiabatic tunneling, originally conceived for one-body problems by Landau, Zener, and Stückelberg (LZS) [9–11]. When a parameter defining the Hamiltonian is varied infinitely slowly (adiabatically), we can just plot a set of energy levels against the parameter, which in general contain level anticrossings, since the two levels should repel with each other unless they are allowed to cross due to, e.g., symmetry reasons. An initial state that starts from one of the lines should evolve with time sticking to that line [adiabatic theorem, corresponding to $p = 0$ in Fig. 3(a)]. When the parameter is varied with a finite velocity, the state can make a transition across the level anticrossing with a finite probability $p[\neq 0$ in Fig. 3(a)], where the transition is caused by a quantum mechanical tunneling across the gap ΔE. The transition probability p depends on the speed the two energy level approach ($\delta\dot{E}$) as

$$p = \exp\left[-2\pi \frac{(\Delta E)^2}{\delta\dot{E}}\right] = \exp\left[-2\pi \frac{(\Delta E)^2}{\frac{d\delta E}{d\Phi} LF}\right]. \quad (3)$$

Here δE is the difference between the "unperturbed," crossing energy levels [dashed lines in Fig. 3(a)] and $\delta\dot{E} \equiv d\delta E/dt = (d\delta E/d\Phi)\dot{\Phi}$ with $LF = d\Phi/dt$. We can immediately see that the process is nonperturbative in F, since p is singular in F.

Although the original LZS theory is devised for one-body systems, there is no reason why we cannot apply it to many-body systems, as demonstrated for a spin system by Miyashita *et al.* [12,13]. So here we apply the concept to the Hubbard model, which is, to our knowledge, the first time the LZS theory is applied to interacting electron systems. In order to check the validity of the LZS picture, we have first calculated the transition probability p. The level anticrossing we focus on is the first one encountered by the ground state at $\Phi = \Phi_0/2$ in the level flow [marked with a double circle in Fig. 3(c)]. In Fig. 4(a) we plot $|\langle\Psi_0|\Psi(t)\rangle|^2$, the weight of the ground state around the level anticrossing, for various values of U and F. From this we have obtained the transition probability p as the asymptotic value of $|\langle\Psi_0|\Psi(t)\rangle|^2$ [14]. Figure 4(b) plots $-\log p$ as a function of the LZS parameter, $(\Delta E)^2/(\delta\dot{E})$, with ΔE now defined as the interaction-originated one. We can see a remarkably accurate linear dependence on the LZS parameter, which clearly indicates that the LZS theory is applicable to the many-body system we have at hand. So the field F and the interaction U enter into the

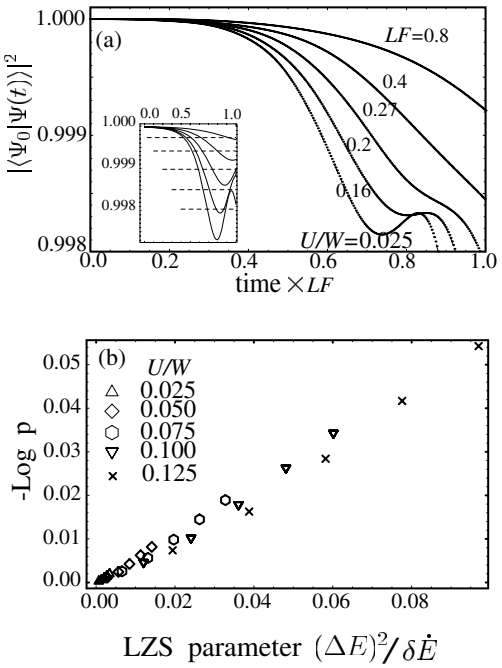

FIG. 4. (a) Time evolution of the weight of the ground state, $|\langle\Phi_0|\Phi(t)\rangle|^2$, calculated for the half-filled Hubbard model ($N = 10, N_\uparrow = N_\downarrow = 5$) for various values of F with $U/W = 0.025$. The inset shows the solutions [14] of the LZS equation with its asymptotic values indicated. (b) Transition probability p (decrease in $|\langle\Phi_0|\Phi(t)\rangle|^2$) plotted against the LZS parameter $[(\Delta E)^2/\delta\dot{E}]$ $[\delta\dot{E} = (d\delta E/d\Phi)LF]$ for various values of F and U/W.

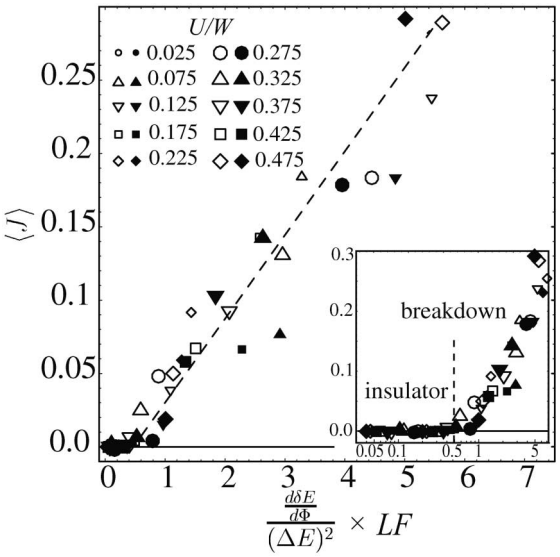

FIG. 5. Time-averaged current plotted against the inverse LZS parameter $(d\delta E/d\Phi)/(\Delta E)^2 \times LF$ for various values of U/W and F in the half-filled Hubbard model with $N = 6$ (open symbols) and $N = 8$ (solid ones). The inset is a blowup of the same data for small F on a log scale.

problem only as a combination $[\Delta E(U)]^2/[(d\delta E/d\Phi)LF]$ [where $\Delta E(U)$ is an increasing function of U; see Fig. 3(b)].

For large enough electric field F the nonadiabatic tunneling is so effective that the state goes straight across each crossing with probability close to unity, so we end up with a long period ($\Delta\Phi = \Phi_0 N$), an analogue of the "extended AB period" discussed for electron systems by Kusakabe and two of the present authors [15,16], a notion originally proposed for a spin (Heisenberg) system by Sutherland [17].

Encouraged by this, we have then replotted the time-averaged current, $\langle J\rangle$, against the inverse of the LZS parameter $(d\delta E/d\Phi)/(\Delta E)^2 \times LF$, in Fig. 5. Dramatically, all of the curves, which appeared quite different for different values of U/W in the raw I-V characteristics (Fig. 2), fall on a single, universal curve within a reasonable error when plotted against the LZS parameter. Specifically, a threshold between the insulating behavior and the dissipative metallic one is clearly seen at around $F \sim 0.5 \times (\Delta E)^2/[(d\delta E/d\Phi)L]$.

After the metallization the current is seen to behave roughly linearly with F, which is surprising, since we have a many-body but clean system. This implies that (i) after many level crossings the system reaches a steady state, and (ii) the many-body gaps at these level crossings have similar magnitudes as the first one (ΔE above). We can in fact recall that the nonadiabatic tunneling is a quantum version of dissipation, where different quantum states become mixed after level anticrossing. Let us examine the nature of the many-body gap $\Delta E(U)$ in the half-filled Hubbard model, which is a charge gap characteristic to the half-filled Hubbard model and vanishes when doped [Fig. 3(c)]. The total momenta of the anticrossing states (the ground state and the excited state with one pair of complex charge rapidities [18]) differ by $2k_F$ where k_F is the Fermi wave number (for small U; replace k_F with the quasimomentum for general U). At half-filling, these umklapp processes take place and the momentum of the many-body state is dissipated. In other words, the role of heat bath degrees of freedom [19] is played by the many-body system itself. Let us add that the current oscillation [typically seen for $LF = 0.008$ in Fig. 1(b)] is due to the kicks from umklapp processes and should be observed in small systems with strong electron correlation. The threshold electric force, $F \simeq 0.5(\Delta E)^2/[(d\delta E/d\Phi)L]$, has a similar order of magnitude as the critical field observed in the experiment [5]. The threshold electric force, $F \sim (\Delta E)^2/[(d\delta E/d\Phi)L]$, should approach an asymptotic value in the thermodynamic limit, since $(d\delta E/d\Phi)|_{\Phi=\Phi_0/2}[\sim(d^2E/d\Phi^2)|_{\Phi=0} \sim$ Drude weight$] \sim 1/L$ should cancel the L in the denominator.

We thank Koichi Kusakabe for discussions, and T. O. acknowledges Naoki Watanabe for a help on the time-dependent numerical simulation.

[1] *Progress in Nonequilibrium Green's Functions*, edited by M. Bonitz (World Scientific, Singapore, 1999).
[2] E. H. Lieb and F. Y. Wu, Phys. Rev. Lett. **20**, 1445 (1968).
[3] T. Fukui and N. Kawakami, Phys. Rev. B **58**, 16 051 (1998).
[4] T. Deguchi *et al.*, J. Phys. A **31**, 7315 (1998).
[5] Y. Taguchi *et al.*, Phys. Rev. B **62**, 7015 (2000).
[6] S. Yamanouchi *et al.*, Phys. Rev. Lett. **83**, 5555 (1999).
[7] Y. Okimoto *et al.*, Science **284**, 1645 (1999).
[8] W. H. Press *et al.*, *Numerical Recipes in Fortran* (Cambridge University Press, Cambridge, 1992), 2nd ed., Sec. 19.2.
[9] L. D. Landau, Phys. Z. Sowjetunion **2**, 46 (1932).
[10] C. Zener, Proc. R. Soc. London A **137**, 696 (1932).
[11] E. C. G. Stückelberg, Helv. Phys. Acta **5**, 369 (1932).
[12] S. Miyashita *et al.*, Phys. Rev. Lett. **80**, 1525 (1998).
[13] H. De Raedt *et al.*, Phys. Rev. B **56**, 11 761 (1997).
[14] We have obtained the asymptotic value of $|\langle\Phi_0|\Phi(t)\rangle|^2$ by fitting the data obtained in Fig. 4(a) to the exact solution [10] $1 - x|D_{-n-1}(z)|^2$ with x as the fitting parameter, where $D_n(z)$ is the Weber function.
[15] K. Kusakabe and H. Aoki, J. Phys. Soc. Jpn. **65**, 2772 (1996).
[16] R. Arita *et al.*, J. Phys. Soc. Jpn. **66**, 2086 (1997).
[17] B. Sutherland, Phys. Rev. Lett. **74**, 816 (1995). See also earlier references on the twisted boundary condition for the XXZ and Hubbard models [B. S. Shastry and B. Sutherland, Phys. Rev. Lett. **65**, 243 (1990); **65**, 1833 (1990)].
[18] F. Woynarovich, J. Phys. C **15**, 85 (1982).
[19] A. O. Caldeira and A. J. Leggett, Ann. Phys. (N.Y.) **149**, 374 (1983).